Formulae for the convolution of $\mathcal{G}^1$ skeleton curves into smooth surfaces

Alvaro Javier Fuentes Suárez, Evelyne Hubert

Formulae for the convolution of $\mathcal{G}^1$ skeleton curves into smooth surfaces

Alvaro Javier Fuentes Suárez*†and Evelyne Hubert‡
Inria Méditerranée, France

1 Introduction

Representation based on skeletons have a major role in interactive modeling and animation of 3D shapes. Skeletons of 3D shapes are made of curves and surfaces, with a preference for the former. Several techniques are used to create a surface enclosing a volume around a skeleton. In this paper we focus on convolution surfaces. This technique provide surfaces with good mathematical features stemming from their definition.

Convolution surfaces are the level sets of a convolution function that results from integrating a *kernel* function K along the *skeleton* $\mathcal{S}$. The mathematical smoothness of the surface obtained depends only on the smoothness of the kernel. The additivity property of integration makes the convolution function independent of the partition of the skeleton. In practice, a kernel function (power inverse, Cauchy, compact support, ...) is selected so as to have closed form expressions for the convolution functions associated to basic skeleton elements (line segments, triangles, ...). Skeletons are then approximated and partitioned into the selected set of basic elements. The convolution function for the whole skeleton is obtained by adding the convolution functions of the constitutive basic elements. See for instance [3, 6, 9, 12, 13, 14, 21, 20, 25, 24].

Line segments are the most commonly used 1D basic skeleton elements. When a skeleton curve has high curvature and torsion, its approximation might require a great number of line segments for the convolution surface to look as intended. In this paper we take the stance that arcs of circles form a very interesting class of basic skeleton elements in the context of convolution. Indeed any space curves can be approximated by circular splines in a $\mathcal{G}^1$ fashion [18, 22]. A lower number of basic skeleton elements are then needed to obtain an appealing convolution surface, resulting into better visual quality at lower computational cost.

To model a wider variety of shapes it is necessary to vary the thickness around the skeleton. Several approaches have been suggested: weighted skeletons [11, 12, 14], varying radius [9], scale invariant integral surfaces [25], the latter two actually providing a more intrinsic formulation. While general closed form formulae were obtained for weighted line segments in [11], there has been a lack of

†alvaro.fuentes-suarez@inria.fr
‡evelyne.hubert@inria.fr
*This project has received funding from the European Union's Horizon 2020 research and innovation programme under the Marie Skłodowska-Curie grant agreement No 675789.

generality in terms of closed form formulae for convolution with varying radius and scale invariant integral surfaces over line segments and, even more so, over arcs of circles. This paper addresses this very issue for the family of power inverse kernels, of even degree.

As initiated in [10, 11], the generality for closed form formulae of the convolution function associated to line segements and arcs of circle for a varying radius or scale is offered in terms of recurrence formulae. Closed form formulae allow eficient evaluation. With recurrence formulae we elegantly reach a higher level of generality: with a simple code we can use kernels of any degree. This contrasts with previous works where the formulae for the convolution functions had to be implemented individually for kernels of each degree. The recurrence formulae in [10, 11] mostly drew on integral functions that appear in some classical tables. An innovative approach is taken in this paper. The recurrence formulae we present in this paper were obtained with the help of Creative Telescoping, an active topic of research in computer algebra. A limited set of pointers is [4, 7, 16] as they provide the background to available software.

In Section 2, we provide the definition of convolution surfaces associated to a skeleton made of curves, with varying thickness. In Section 3 we examine the convolution of line segments, providing the closed form formulae for the convolution functions, with varying thickness. In Section 4 we turn to arcs of circles. In Section 5 we demonstrate the interest of having arcs of circles as basic skeleton elements for convolution and discuss future directions.

2 Convolution surfaces

In this section we recall the basics of convolution surfaces. We first discuss families of kernels that arose in computer graphics literature. Thereafter, we shall mainly focus on the family of *power inverse* kernels. We then define convolution function generated by bounded regular curves and the alternative definitions of convolution that allow to generate shapes with varying thickness around the skeleton.

2.1 Kernels

The kernels in use in the literature are given by functions $K : \mathbb{R}^+ \to \mathbb{R}^+$ that are at least continuously differentiable. The argument is the distance between a point in space and a point on the skeleton. Those kernels are decreasing functions on $\mathbb{R}^+$ and strictly decreasing when non zero: $K(r) > 0 \Rightarrow K'(r) < 0$.

The first convolution surfaces that appeared in computer graphics [2, 3] were based on the Gaussian kernel: $r \mapsto e^{-s\,r^2}$ that depends on a parameter $s > 0$. The difficulty in evaluating the resulting convolutions prompted the introduction of kernels that provided closed form expressions for the convolution functions associated to basic skeleton elements. [20, 21] promoted the Cauchy kernel $r \mapsto \frac{1}{(1+\sigma\,r^2)^2}$ after [23] introduced the inverse function $r \mapsto \frac{1}{r}$. For faster convolution [9, 6] introduced the power inverse cube kernel $r \mapsto \frac{1}{r^3}$. [12] also exhibited the benefit of using the quintic inverse $r \mapsto \frac{1}{r^5}$.

This paper is mostly concerned with the family of power inverse kernels. They are indexed by $i \in \mathbb{N} \setminus \{0\}$ and given by

$$\boldsymbol{p}^i : r \mapsto \left(\frac{1}{r}\right)^i$$

The convolution surfaces obtained with a power inverse kernel always enclose the skeleton since these functions tend to infinity when approaching the skeleton. As exploited in [11, 10] the closed form formulae of convolution functions using the family of Cauchy kernels $\boldsymbol{c}^i_\sigma : r \mapsto \left(\frac{1}{1+\sigma r^2}\right)^{\frac{i}{2}}$ differ only slightly from the ones using power inverse kernels.

The power inverse kernels decrease relatively fast with distance but have an infinite support and can lead to unwanted bulges or blending (Figure 3). Kernels with compact support allow to avoid these to some extent as a given point on the skeleton has a finite radius R of influence. A family of compact support kernels is indexed by $i \in \mathbb{N} \setminus \{0\}$ and given by

$$\boldsymbol{k}^i_R : r \mapsto \begin{cases} \left(1 - \left(\frac{r}{R}\right)^2\right)^{\frac{i}{2}} & \text{if } r < R \\ 0 & \text{otherwise.} \end{cases}$$

Their use necessitates to determine the geometry of the intersection of the skeleton with spheres. To obtain convolution surfaces that are at least continuously differentiable we consider only $\boldsymbol{k}^i_R$ for $i \geq 3$. For $i < 3$, $\boldsymbol{k}^i_R$ is not differentiable at $r = R$. The case $i = 4$ is actually the case considered in [15, 21]. As we increase i though, we obtain smoother shapes.

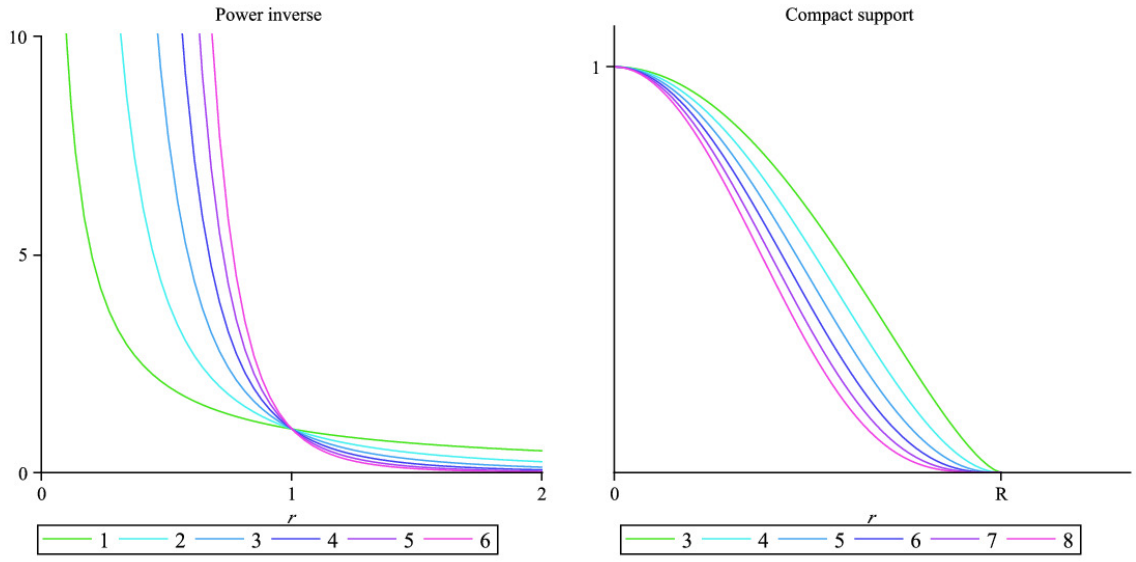

Figure 1: The graphs of the kernel functions $\boldsymbol{p}^i$ and $\boldsymbol{k}^i_R$, varying i.

2.2 Notations

Typically $P = (p_1, p_2, p_3)^T \in \mathbb{R}^n$ represents a point in space and $A = (a_1, a_2, a_3)^T$, $B = (b_1, b_2, b_3)^T$ represent the end points of a line segment $[AB]$ or arc of circle $\widehat{AOB}$ with center O. The

straight line through A and B is denoted as (AB). Then $\overrightarrow{AP}$ represent the vector from A to P. In the following $\overrightarrow{u} = (u_1, u_2, u_3)^T$, $\overrightarrow{v} = (v_1, v_2, v_3)^T \in \mathbb{R}^n$ also represent vectors. The scalar product of two vectors $\overrightarrow{u} = (u_1, u_2, u_3)^T$ and $\overrightarrow{v} = (v_1, v_2, v_3) \in \mathbb{R}^n$ is then $\overrightarrow{u} \cdot \overrightarrow{v} = u_1v_1 + u_2v_2 + u_3\, v_3$. The distance between two points A and B is denoted as $|AB| = \sqrt{(b_1 - a_1)^2 + (b_2 - a_2)^2 + (b_3 - a_3)^2}$

2.3 Convolution of regular curves

We assume here that the *skeleton* can be partitioned into *regular patches* defined by bounded regular curves parametrized by an interval $[a, b]$ of $\mathbb{R}$. The convolution function for the skeleton is then obtained by summing the convolution functions for each of those patches.

Consider first a parametrized curve $\Gamma : [a, b] \subset \mathbb{R} \to \mathbb{R}^3$. It is a regular curve if Γ is continuously differentiable and Γ' doesn't vanish. The infinitesimal arc-length is $|\Gamma'(t)|\,\mathrm{d}t$. The convolution function based on $\mathcal{S} = \Gamma([a, b])$ at a point $P \in \mathbb{R}^3$ is then defined by

$$\mathcal{C}^K_\Gamma(P) = \int_a^b K\left(|P\Gamma(t)|\right)\, |\Gamma'(t)|\mathrm{d}t.$$

The integral is independent of the (regular) parametrization of the curve used. Convolution functions with a power inverse kernel $K = \boldsymbol{p}^i$ are infinitely differentiable outside of the curve $\Gamma([a, b])$. Convolution functions with a compact support kernel $K = \boldsymbol{k}^i_R$ are $\lfloor \frac{i-1}{2} \rfloor$ continuously differentiable.

As the reverse image of a closed set by a k-continuously differentiable map, $k \geq 1$, the resulting *convolution surfaces* $\left\{P \in \mathbb{R}^3 \,|\, \mathcal{C}^K_\Gamma(P) = \kappa\right\}$ are closed (in a topological sense) and smooth, provided κ is not a critical value* of $\mathcal{C}^K_\Gamma$. It is the boundary of a smooth 3-dimensional manifold $V_\kappa = \left\{P \in \mathbb{R}^3 \,|\, \mathcal{C}^K_\Gamma(P) \geq \kappa\right\}$. Furthermore V_κ and $V_{\kappa'}$ are diffeomorphic provided that there is no critical values in the interval $[\kappa, \kappa']$ [17, Theorem 3.1]. With the power inverse kernel, the skeleton is in V_κ for any $\kappa > 0$. This is not always the case with a compact support kernel; V_κ can even be the empty set for too high values of κ.

2.4 Discussion on the choice of a kernel

With compact support kernels $\boldsymbol{k}^i_R$ the smoothness of the convolution surface increases with i. With power inverse kernels $\boldsymbol{p}^i$ the convolution functions are smooth at all points outside the skeleton. Yet, as i increases, the convolution surface is *sharper* around the skeleton. This is illustrated in Figure 2.

When the convolution function has a critical point, chances are that there is a change in the topology of the convolution surface as it goes through the critical value [17]. This is illustrated in Figure 3 with a skeleton made of two line segments. The convolution function has a critical point and the convolution surface through this point has a singularity. The corresponding level set is a transition from bulging to blending, from two connected components to a single component. Figure 3 also illustrates the fact that compact support kernels allow to dismiss the influence of skeleton elements that are at distance more than R, thus avoiding some of the bulging and blending that appear for the kernels with infinite support kernel.

*A critical point of a function $f : (x, y, z) \mapsto f(x, y, z)$ is a point (x_0, y_0, z_0) at which the gradient (f_x, f_y, f_z) of f vanishes. A critical value of f is the value $f(x_0, y_0, z_0)$ of f at a critical point (x_0, y_0, z_0).

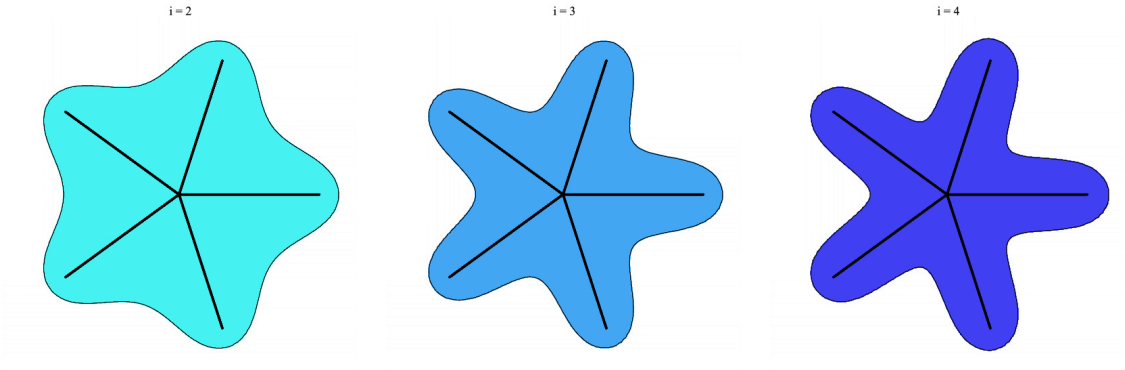

Figure 2: Convolution curves for a set of segments with power inverse kernel $\boldsymbol{p}^2$, $\boldsymbol{p}^3$, $\boldsymbol{p}^4$. The convolution function for the whole set is obtained as the sum of the convolution functions for each line segment. The level set is adapted to have identical thickness at the tips. Note that sharpness increases from left to right.

2.5 Varying thickness

Several alternatives have been introduced for varying the thickness of the convolution surface along the skeleton. A first idea was to use a *weight* function along the skeleton. For a skeleton given by a regular curve $\Gamma : [a, b] \to \mathbb{R}^3$, one uses a weight function $w : [a, b] \to \mathbb{R}$. The convolution function is then defined as

$$\mathcal{C}^K_{\Gamma,w}(P) = \int_a^b w(t) K\left(|P\Gamma(t)|\right) \, |\Gamma'(t)| \, \mathrm{d}t.$$

The convolution function is now dependent on the parametrization used for the skeleton curve. Polynomial weight functions are used in [11, 12, 13, 14]. The drawback of this approach was illustrated in [11, Figure 9]: the influence of the weight diminishes as the degree of the kernel increases. Alternative more intrinsic formulations were proposed in [9] and [25].

2.5.1 Varying radius as proposed by Hornus *et al.* [9]

In [9] Hornus *et al.* proposed a different way of computing the convolution function. This allows the user to modify the shape of the final surface according to a radius assigned to each point in the skeleton: the distance is divided by the radius at the corresponding point in the skeleton. For a skeleton curve $\Gamma : [a, b] \to \mathbb{R}^3$ the radius is given by a function $\rho : [a, b] \to \mathbb{R}^+$. The convolution function is then defined by

$$\mathcal{H}^K_{\Gamma,\rho}(P) = \int_a^b K\left(\frac{|P\Gamma(t)|}{\rho(t)}\right) \, |\Gamma'(t)| \, \mathrm{d}t.$$

If additional precaution are not imposed on the radius function ρ, this convolution function is not independent of the parametrization of the curve Γ. In practice it makes sense to have a radius function that is approximately linear in the arc-length.

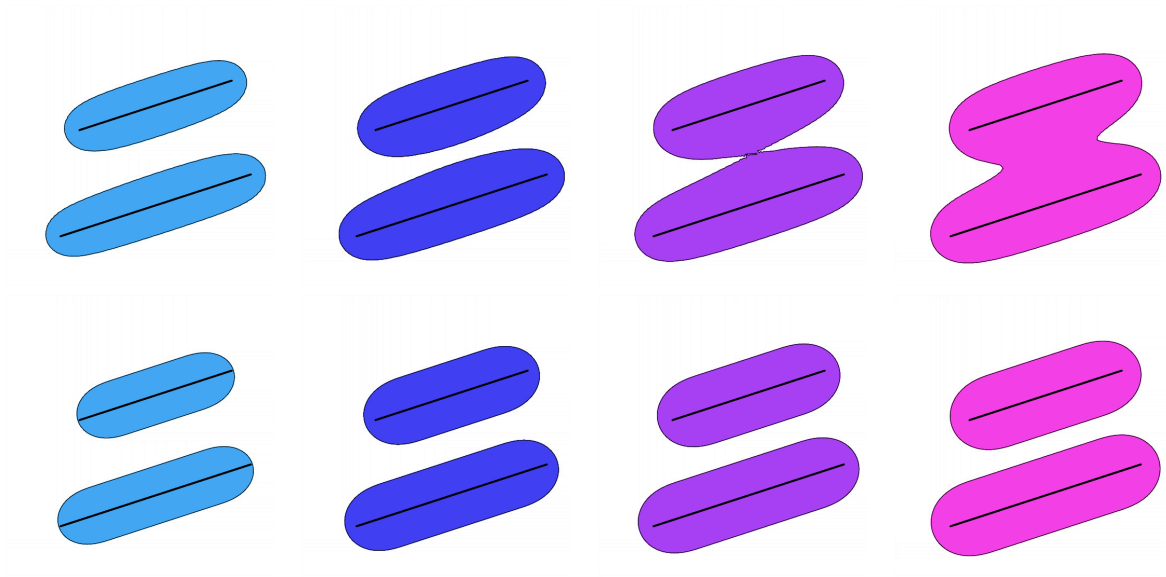

Figure 3: Convolution curves based on two parallel segments. The top line uses the cubic inverse kernel $\boldsymbol{p}^3$ and the bottom line a compact support kernel $\boldsymbol{k}_R^3$. Columns correspond to an identical sought thickness. For the cubic inverse kernel, a bulge and then a blend appear between the line segments, while the convolution surfaces get only thicker with the compact support kernel.

2.5.2 SCALIS as proposed by Zanni *et al.* [25]

An alternative convolution introduced in [25] allows to properly model shapes with pieces at different scales. For a regular curve $\Gamma : [a, b] \subset \mathbb{R} \to \mathbb{R}^3$, the SCALIS convolution function is

$$\mathcal{S}^K_{\Gamma,\lambda}(P) = \int_a^b K\left(\frac{|P\Gamma(t)|}{\lambda(t)}\right) \frac{|\Gamma'(t)|}{\lambda(t)}\,\mathrm{d}t,$$

where $\lambda : [a, b] \to \mathbb{R}^+$ is called the *scale function*. Notice that λ plays a similar role as ρ in the formulation by Hornus. To apprehend all the good features of this new definition of convolution surface, the reader is referred to [25, 24]. Let us just observe the case where λ is a constant. If we write $\lambda \cdot P$ and $\lambda \cdot \Gamma$ for the point and the regular curve obtained through a homothety (*a.k.a* homogeneous dilatation or scaling) with ratio λ, then

$$\mathcal{S}^K_{\lambda\cdot\Gamma,\lambda}(\lambda \cdot P) = \mathcal{C}^K_\Gamma(P) \quad \text{or equivalently} \quad \mathcal{S}^K_{\Gamma,\lambda}(P) = \mathcal{C}^K_{\lambda^{-1}\cdot\Gamma}\left(\lambda^{-1} \cdot P\right).$$

This implies that the convolution surface of equation $\mathcal{S}^K_{\lambda\cdot\Gamma,\lambda}(P) = c$ is homothetic to the convolution surface $\mathcal{C}^K_\Gamma(P) = c$ with a ratio λ.

3 Convolution with line segments

We examine the convolution of line segments for power inverse kernels, with varying radius or varying scale*. First we express the convolution functions, with varying radius or scale, in terms of

*Results for convolution of weighted line segments with power inverse and Cauchy kernels can be found in [11].

an integral function indexed by two integers:

$$\boldsymbol{I}_{i,k}(a,b,c,\lambda,\delta) = \int_{-1}^{1} \frac{(\lambda+\delta\,t)^k}{(a\,t^2-2\,b\,t+c)^i} dt$$

We then provide recurrence formulae on this integral so as to have all the convolution functions for line segments with (even) power inverse kernels. The recurrence relationships we exhibit can be adapted to work for all powers. Furthermore, though we do not give details, these recurence also allows to deal with the convolution of line segments with the family of compact support kernels. We choose to restrict here to even powers as they provide easier formulae to evaluate (odd power inverse kernels bring out elliptic functions in the convolution of arcs of circles and planar polygons). This does not affect too much the variety of shapes we can obtain.

3.1 Integrals for convolution

Two points $A, B \in \mathbb{R}^3$ define the line segment $[AB]$. A regular parametrization for this line segment is given by $\Gamma : [-1,1] \to \mathbb{R}^3$ with $\Gamma(t) = \frac{A+B}{2} + \frac{B-A}{2}\,t$. Therefore for a point $P \in \mathbb{R}^3$ we have

$$4\,|P\Gamma(t)|^2 = |AB|^2\,t^2 - 2\,\overrightarrow{AB}\cdot\overrightarrow{CP}\,t + |CP|^2 \text{ where } C = \frac{A+B}{2}$$

is the mid point of the line segment $[AB]$. Hence $|\Gamma'(t)| = \frac{|AB|}{2}$.
The simple convolution of this line segment with the power inverse kernel $\boldsymbol{p}^{2i}$ is thus given by:

$$\mathcal{C}^{2i}_{[AB]}(P) = \frac{|AB|}{2}\int_{-1}^{1} \frac{1}{|P\Gamma(t)|^{2i}}\,\mathrm{d}t = \frac{|AB|}{2}\,\boldsymbol{I}_{i,0}\left(\frac{1}{4}|AB|^2,\,\frac{1}{4}\overrightarrow{AB}\cdot\overrightarrow{CP},\,\frac{1}{4}|CP|^2,\lambda,\delta\right).$$

If we choose the radius function $\rho : [a,b] \to \mathbb{R}$ to be linear in the arclength we can find $\lambda, \delta \in \mathbb{R}$ such that $\rho(t) = \lambda + \delta t$. Convolution with varying radius is then given by:

$$\mathcal{H}^{2i}_{[AB],\rho}(P) = \int_{-1}^{1} \frac{(\lambda+\delta\,t)^{2i}}{|P\Gamma(t)|^{2i}}\,\frac{|AB|}{2}\mathrm{d}t = \frac{|AB|}{2}\,\boldsymbol{I}_{i,2i}\left(\frac{1}{4}|AB|^2,\,\frac{1}{4}\overrightarrow{AB}\cdot\overrightarrow{CP},\,\frac{1}{4}|CP|^2,\,\lambda,\,\delta\right).$$

If we now take the scale function to be $\Lambda(t) = \lambda + \delta t$, then

$$\mathcal{S}^{2i}_{[AB],\Lambda}(P) = \int_{-1}^{1} \frac{(\lambda+\delta\,t)^{2i}}{|P\Gamma(t)|^{2i}}\,\frac{|AB|}{2(\lambda+\delta\,t)}\mathrm{d}t = \frac{|AB|}{2}\,\boldsymbol{I}_{i,2i-1}\left(\frac{1}{4}|AB|^2,\,\frac{1}{4}\overrightarrow{AB}\cdot\overrightarrow{CP},\,\frac{1}{4}|CP|^2,\,\lambda,\,\delta\right).$$

3.2 Closed forms through recurrence formulae

First of all, given that

$$\boldsymbol{I}_{1,0}(a,b,c,\lambda,\delta) = \frac{1}{\sqrt{ac-b^2}}\,\left[\arctan\left(\frac{a\,t-b}{\sqrt{ac-b^2}}\right)\right]_{-1}^{1}$$

we can determine $\boldsymbol{I}_{i,0}(a,b,c,\lambda,\delta)$ for all $i \geq 1$ thanks to the recurrence relationship

$$2\,i\left(ac-b^2\right)\boldsymbol{I}_{i+1,0} + (1-2\,i)\,a\,\boldsymbol{I}_{i,0} = \left[\frac{at-b}{(at^2-2\,bt+c)^i}\right]_{-1}^{1}.$$

One then observes that:

$$2\,a\,(1-i)\,\boldsymbol{I}_{i,1} = 2\,(3-i)\,(a\lambda+b\delta)\,\boldsymbol{I}_{i,0} + \left[\frac{\delta}{(at^2-2\,bt+c)^{i-1}}\right]_{-1}^{1}$$

This recurrence is actually obtained by specializing the following recurrence to $k=-1$

$$a\,(k-2\,i+3)\,\boldsymbol{I}_{i,k+2}+2\,(i-2-k)\,(a\lambda+b\delta)\,\boldsymbol{I}_{i,k+1}+(k+1)\left(a\lambda^2+c\delta^2+2\,b\lambda\,\delta\right)\boldsymbol{I}_{i,k} = \left[\frac{\delta\,(\lambda+\delta\,t)^{k+1}}{(at^2-2\,bt+c)^{i-1}}\right]_{-1}^{1}$$

One can thus determine $\boldsymbol{I}_{i,k}$ for all $i\geq 1$ and $k\geq 0$ and therefore $\boldsymbol{I}_{i,2i}$ and $\boldsymbol{I}_{i,2i-1}$ that are needed for convolution with varying radius or scale.

Alternatively, to determine the convolution with varying radius, we can consider the recurrence

$$2\,i\,(i+1)\,a\left(ac-b^2\right)\boldsymbol{I}_{i+2,2i+4} - i\left(\lambda\,a\,(1+2\,i)\,(2\,b\delta+a\lambda)+\left((4\,i+5)ca-2\,(i+2)b^2\right)\delta^2\right)\boldsymbol{I}_{i+1,2i+2}$$

$$+\delta^2(i+1)(1+2\,i)\left(a\lambda^2+c\delta^2+2\,b\lambda\,\delta\right)\boldsymbol{I}_{i,2i} = \left[\frac{(\lambda+\delta\,t)^{2\,i+1}}{(at^2-2\,bt+c)^{i+1}}\,C\right]_{-1}^{1}$$

where

$$\begin{array}{rcl} C & = & \left(\left(ac+2\,b^2i\right)t^2-bc\,(3\,i+2)\,t+c^2\,(i+1)\right)\delta^3 \\ & & +\left(2\,ab\,(1+2\,i)\,t^2-\left(2\,(i+2)\,b^2+3\,aic\right)t+bc\,(i+2)\right)\lambda\,\delta^2 \\ & & +\left(a^2\,(1+2\,i)\,t^2-ab\,(i+2)\,t-ac\,(i-1)\right)\lambda^2\delta+ai\,(at-b)\,\lambda^3 \end{array}.$$

A similar recurrence can be obtained for $\boldsymbol{I}_{i,2i-1}$. As the previous ones, it is obtained by Creative Telescoping. We have mostly used `Mgfun`* by F. Chyzak (in Maple) but we have also tried `HolonomicFunctions`* by C. Koutschan (in Mathematica).

4 Convolution with arcs of circle

We examine the convolution of an arc of circle for power inverse kernels. Though arcs of circles appear in the literature about convolution surfaces [13, 26], there is no general formulae for these. In this section we choose a parametrization for arcs of circle that allows us to write the convolution functions (with varying radius or scale) in terms of an integral indexed by two integers:

$$\boldsymbol{F}_{i,k}(a,b,c,\lambda,\delta) = \int_{-T}^{T}\frac{(\lambda+\delta\,t)^k\,(t^2+1)^{i-1}}{(a\,t^2-2\,b\,t+c)^i}dt$$

We then show how to determine closed form formula for these integrals thanks to some recurrences. We restrict our attention to convolution of arcs of circle with even power inverse kernels. With odd power inverse kernels, the closed form formulae for the convolution function involve elliptic functions and can be rather impractical to evaluate.

*https://specfun.inria.fr/chyzak/mgfun.html

*http://www.risc.jku.at/research/combinat/software/ergosum/RISC/HolonomicFunctions.html

The closed form formulae for the convolution of arcs of circle with the family of compact support kernels are challenging to obtain. The software `MixedCT`* by L. Dumont (in Maple) does meet this challenge. The result would be too cumbersome to be presented here and it is not clear at this stage how to use it efficiently.

4.1 Rational parametrization

When it comes to integration, rational functions are the dependable class [5]. The main ingredient in obtaining closed-form convolution primitives for arcs of circle is to introduce an appropriate rational parametrization.

We assume that the points O, A and B are not aligned and such that $|OA| = |OB| = r$. They define a plane in space and two arcs of circle, one of angle α the other of angle $\pi + \alpha$ for some $0 < \alpha < \pi$. We have

$$\alpha = \arccos\left(\frac{\overrightarrow{OA} \cdot \overrightarrow{OB}}{r^2}\right) \qquad \text{with} \quad 0 < \alpha < \pi$$

and accordingly to which angle is dealt with we set

$$T = \tan\left(\frac{\alpha}{4}\right) \quad \text{or} \quad T = \tan\left(\frac{\pi + \alpha}{4}\right).$$

Momentarily we consider the coordinate system (x, y, z) where the origin is the center of the circle, the x-axis is the bisector of the chosen angle defined by O, A and B and the (x, y) plane is the plane of the circle. See Figure 4.

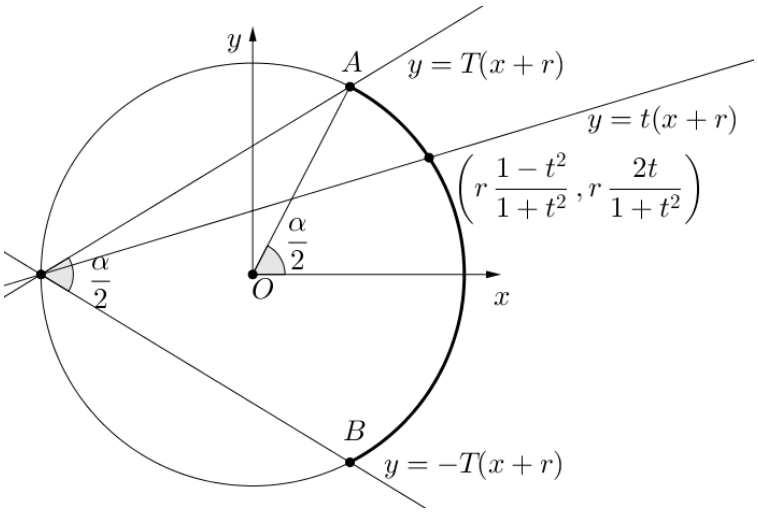

Figure 4: Rational parametrization of an arc of circle.

A parametrization of the arc of circle is then given by

$$\begin{array}{rccc} \Gamma: & [-T, T] & \longrightarrow & \mathbb{R}^3 \\ & t & \mapsto & \left(r\,\dfrac{1-t^2}{t^2+1}, r\,\dfrac{2\,t}{t^2+1}, 0\right). \end{array}$$

*http://mixedct.gforge.inria.fr

This is obtained by determining the intersection of the circle with the lines of slope t through the point diametrically opposite to the middle of the arc. Consider a point $P = (x, y, z)$ in space. We have

$$|P\Gamma(t)|^2 = \frac{\alpha t^2 - 2\,\beta\,t + \gamma}{t^2+1} \quad \text{where} \quad \alpha = (x+r)^2 + y^2 + z^2, \quad \beta = 2\,r\,y, \quad \gamma = (x-r)^2 + y^2 + z^2.$$

Note that

$$\begin{aligned} \gamma + \alpha &= 2\,(|OP|^2 + r^2) \\ \alpha\,T^2 + 2\,\beta\,T + \gamma &= (T^2+1)\,|AP|^2 \\ \gamma\,T^2 - 2\,\beta\,T + \gamma &= (T^2+1)\,|BP|^2 \end{aligned}$$

so that (α, β, γ) is actually the solution of a linear system that depends on T and the squares of the distances of P to O, A and B. There is a unique solution provided that A, O and B are not aligned, i.e. $T(T^2-1) \neq 0$. This solution is:

$$\alpha = \frac{\left(|PA|^2 + |PB|^2\right)(T^2+1) - 4\,(|PO|^2 + r^2)}{T^2-1}$$

and

$$\beta = \frac{\left(|PA|^2 - |PB|^2\right)(T^2+1)}{T} \quad \gamma = 2\,\left(|PO|^2 + r^2\right) - \alpha.$$

4.2 Integrals for convolution

Using the above parametrization of an arc of circle $\widehat{A^OB}$ the associated convolution function with the power inverse kernel $\boldsymbol{p}^{2i}$ is

$$\mathcal{C}^{2i}_{\widehat{A^OB}}(P) = \int_{-T}^{T} \frac{1}{|P\Gamma(t)|^{2i}} \frac{2\,r}{1+t^2}\mathrm{d}t = 2\,r\,\int_{-T}^{T} \frac{(1+t^2)^{i-1}}{(\alpha t^2 - 2\,\beta\,t + \gamma)^i}\mathrm{d}t = 2\,r\,\boldsymbol{F}_{i,0}\,(\alpha, \beta, \gamma, \lambda, \delta)$$

as the infinitesimal arclength is $|\Gamma'(t)| = \frac{2r}{1+t^2}$.

We choose a radius or scale function $\rho, \Lambda : [-T, T] \to \mathbb{R}$ that is linear in the parameter t used above. A more intrinsic choice would be to have a radius or scale function linear in the arc length. Since the arclenth is $2r\arctan(t) \sim 2\,r\,t + O(t^3)$, linearity in t is a reasonable approximation for arcs defined by an angle less than π. This is illustrated in Figure 5.

Convolution with varying radius according to $\rho : t \mapsto \lambda + \delta\,t$ is then given by:

$$\mathcal{H}^{2i}_{\widehat{A^OB},\rho}(P) = \int_{-T}^{T} \frac{(\lambda + \delta\,t)^{2i}}{|P\Gamma(t)|^{2i}} \frac{2\,r}{1+t^2}\mathrm{d}t = 2\,r\,\boldsymbol{F}_{i,2i}\,(\alpha, \beta, \gamma, \lambda, \delta)\,.$$

Convolution with scale function $\Lambda : t \mapsto \lambda + \delta\,t$ is given by:

$$\mathcal{S}^{2i}_{\widehat{A^OB},\Lambda}(P) = \int_{-T}^{T} \frac{(\lambda + \delta\,t)^{i}}{|P\Gamma(t)|^{i}} \frac{2\,r}{1+t^2} \frac{\mathrm{d}t}{1+\delta\,t} = 2\,r\,\boldsymbol{F}^{-T,T}_{i,i-2,i-1}\,(\alpha, \beta, \gamma, \lambda, \delta)\,.$$

4.3 Closed forms through recurrence formulae

Given that

$$\boldsymbol{F}_{1,0} = \left[\frac{1}{\sqrt{ca-b^2}}\arctan\left(\frac{a\,t-b}{\sqrt{ca-b^2}}\right)\right]_{-T}^{T}$$

we can recover the expression for $\boldsymbol{F}_{i,0}$, for all $i \in \mathbb{N}$, thanks to the recurrence relationship

$$2\,(i+1)\left(ac-b^2\right)\boldsymbol{F}_{i+2,0} - (1+2\,i)\,(a+c)\,\boldsymbol{F}_{i+1,0} + 2\,i\,\boldsymbol{F}_{i,0} = \left[\frac{\left(1+t^2\right)^i\left(b\left(t^2-1\right)+(a-c)\,t\right)}{\left(at^2-2\,bt+c\right)^{i+1}}\right]_{-T}^{T}$$

On the other hand, the integrals $\boldsymbol{F}_{i,k}$ satisfy the following recurrence:

$$a\,(k+3)\,\boldsymbol{F}_{i,k+4} - A_3\,\boldsymbol{F}_{i,k+3} + A_2\,\boldsymbol{F}_{i,k+2} + A_1\,\boldsymbol{F}_{i,k+1} + A_0\,(k+1)\,\boldsymbol{F}_{i,k} = \left[\frac{\delta^3\left(1+t^2\right)^i(\lambda+\delta\,t)^{k+1}}{\left(at^2-2\,bt+c\right)^{i-1}}\right]_{-T}^{T}$$

where

$$\begin{aligned}
A_3 &= -2\,(2\,k+5)\,a\lambda - 2\,b\,(i+2+k)\,\delta,\\
A_2 &= 6\,(k+2)\,a\lambda^2 + 2\,b\,(5+3\,k+2\,i)\,\delta\,\lambda + ((3+k-2\,i)\,a + (k+2\,i+1)\,c)\,\delta^2,\\
A_1 &= -2\,a\,(3+2\,k)\,\lambda^3 - 2\,b\,(4+3\,k+i)\,\delta\,\lambda^2 + 2\,((i-2-k)\,a - (i+1+k)\,c)\,\delta^2\lambda + 2\,b\,(i-2-k)\,\delta^3,\\
A_0 &= \left(\delta^2+\lambda^2\right)\left(\lambda^2 a + c\delta^2 + 2\,b\lambda\,\delta\right).
\end{aligned}$$

By specializing the above equation to $k=-1$ one can obtain $\boldsymbol{F}_{i,3}$ from $\boldsymbol{F}_{i,2}$, $\boldsymbol{F}_{i,1}$ and $\boldsymbol{F}_{i,0}$. These latter are thus sufficient to determine $\boldsymbol{F}_{i,k}$ for all $k \geq 4$.

To determine $\boldsymbol{F}_{i,1}$ we observe that, for $i \neq 0$,

$$a\,\boldsymbol{F}_{i+1,1} - \boldsymbol{F}_{i,1} = (b\,\delta + a\,\lambda)\,\boldsymbol{F}_{i+1,0} - \lambda\,\boldsymbol{F}_{i,0} - \frac{\delta}{2\,i}\left[\frac{\left(1+t^2\right)^{\frac{i}{2}}}{\left(at^2-2\,bt+c\right)^{\frac{i}{2}}}\right]_{-T}^{T}$$

and

$$\boldsymbol{F}_{1,1} = \left[\frac{(b\,\delta+a\,\lambda)}{a\sqrt{ac-b^2}}\arctan\left(\frac{at-b}{\sqrt{ac-b^2}}\right) + \frac{\delta}{2a}\,\ln\left(at^2-2\,bt+c\right)\right]_{-T}^{T}.$$

To determine $\boldsymbol{F}_{i,2}$ we can use the linear recurrence that provides $\boldsymbol{F}_{i,k+1}$ in terms of $\boldsymbol{F}_{i,k+1}$, $\boldsymbol{F}_{i,k}, \boldsymbol{F}_{i+1,k}$, and $\boldsymbol{F}_{i+2,k}$. Specialized to $k=0$ this recurrence simplifies to:

$$A_{02}\,\boldsymbol{F}_{i,2} + A_{01}\,\boldsymbol{F}_{i,1} + A_{00}\,\boldsymbol{F}_{i,0} + A_{10}\,\boldsymbol{F}_{i+1,0} + A_{20}\,\boldsymbol{F}_{i+2,0} = \left[\delta\,\frac{(\lambda+\delta\,t)\left(1+t^2\right)^i}{\left(at^2-2\,bt+c\right)^{i+1}}\,C\right]_{-T}^{T}$$

where

$$\begin{aligned}
A_{02} &= a\left((a-c)\,\delta\,\lambda + b(\delta^2-\lambda^2)\right),\\
A_{01} &= -2\,(ib\delta + \lambda\,a)\left(-\lambda^2 b + (a-c)\,\delta\,\lambda + b\delta^2\right),\\
A_{00} &= -\left(\delta^2+\lambda^2\right)\left(b\left((2\,i-1)\,a + 2\,ci\right)\delta^2 + \left((2\,i-1)\,a^2 + ac + 2\,b^2 i\right)\lambda\,\delta + \lambda^2 ab\right),\\
A_{10} &= (1+2\,i)\,a^2\,(a+c)\,\delta\,\lambda^3 + b\left(3\,a^2\,(1+2\,i) + ac\,(3+4\,i) + 2\,ib^2\right)\delta^2\lambda^2\\
&\quad + \left((4\,i+1)\,ca^2 + a\left(c^2 + 2\,b^2\,(i+1)\right) + 2\,b^2\,(3\,i+1)\,c\right)\delta^3\lambda + \; b\left((4\,i+1)\,ca + (1+2\,i)\,c^2 - 2\,ib^2\right)\delta^4,\\
A_{20} &= -2\,\delta\,(i+1)\,(\lambda\,a + b\delta)\left(ac-b^2\right)\left(a\lambda^2 + c\delta^2 + 2\,b\lambda\,\delta\right),
\end{aligned}$$

and

$$\begin{aligned} C &= a^2\left(b-bt^2-(a-c)\,t\right)\lambda^2+\left(a^2bt^2-b^2\,(3\,a+c)\,t+b\left(c^2+2\,b^2\right)\right)\delta^2 \\ &\quad +\left(a^2\,(a-c)\,t^2-2\,b\left(b^2+2\,a^2-ac\right)t+b^2\,(3\,a+c)\right)\delta\,\lambda. \end{aligned}$$

5 Application and outlook

The formulae presented above were used to compute some examples.

Figure 5 shows the convolution with a varying radius of a line segment and four arcs of circles. The skeleton curves all have the same extremeties but different radius. The angle supporting the arc of circle thus varies. Only when this angle is close to 2π does one detect that the thickness does not vary linearly with the arc length.

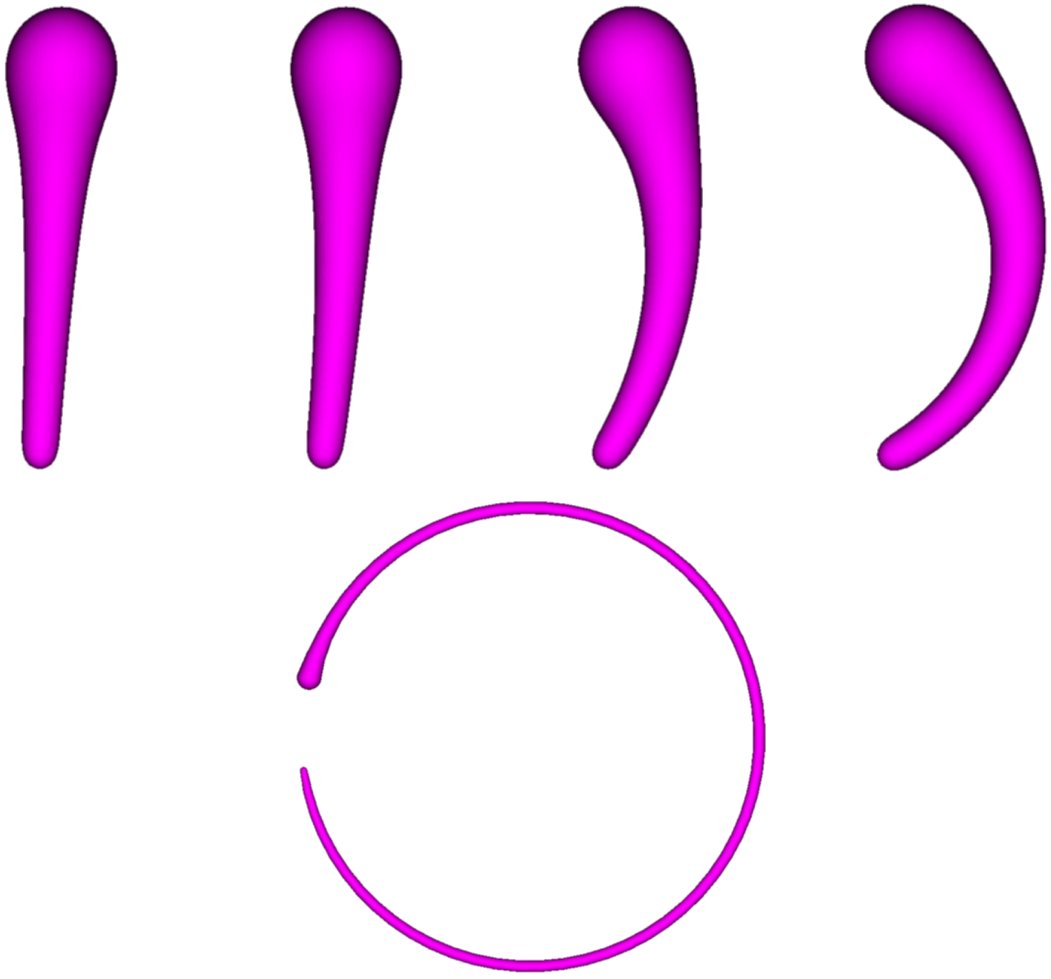

Figure 5: Convolution with varying radius for a line segment (top left) and arcs of circles supported respectively by an angle $\frac{\pi}{24}$, $\frac{\pi}{3}$, $\frac{2\pi}{3}$ and $\frac{19\pi}{10}$ (bottom, with a different scale).

We can combine several arcs of circles and line segments to model $\mathcal{G}^1$curves to serve as skeleton.

This is illustrated for two closed curves in Figure 6.

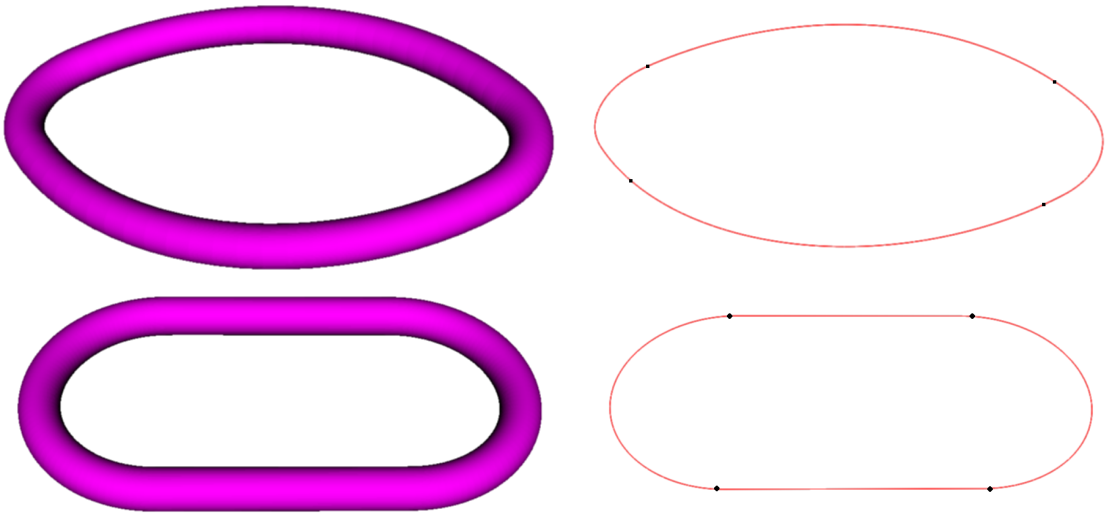

Figure 6: Convolution surface modeling a smooth chain ring. Top row: modeling with arcs only; bottom: arcs and segments. Left image: the surface; right: the skeleton composed of only 4 arcs; in black the joint points.

The widely used approach for more elaborate skeleton curves is to use an approximation by line segments [6, 9, 14, 21, 25]. An issue with this versatile approach is that either the resulting convolution surface presents some visible turns at the joints of line segments, or the number of segments must be increased significantly in order to get a visually smooth surface. Convolution for arcs of circles were also examined in [13, 26], in particular for the possible deformations into helices that have powerful modeling properties for the animation of hair [1]. The warping technique used in [26] allows to decrease substantially the number of skeleton basic elements to be used to obtain a natural looking shape. This provides a substantial gain on the computational cost as the visualization of the surface requires the repeated evaluation of the convolution function. Yet the surfaces obtained by warping in [26] exhibit artifacts and singularities so that this technique requires a fine tuning of the warping parameters.

The alternative approach we want to bring forth in this paper is to use a $\mathcal{G}^1$-approximation of the skeleton curve. Arcs of circles have the great advantage to allow the construction of $\mathcal{G}^1$-curves that can approximate any curve [18, 22]. One can thus achieve both mathematically smooth and visually appealing shapes with skeleton curves consisting of few basic elements. This improves visual quality and decreases the computational cost. Figures 7,8 and 9 compare the convolution surfaces with skeleton curves generated with arcs of circle and line segments. The visual quality of the surface is obtained with much fewer arcs of circles rather than line segments.

Conclusion: In this paper we have focused on convolution surfaces along skeleton consisting of a single curve, either open or closed. We propose to use approximation by line segments and arcs of circles to approximate this curve so as to obtain quality convolution surfaces with lower computational cost. To this effect we provided explicit formulae for the convolution functions for both line segments and arcs of circles, with varying radii or scale functions. These formulae have

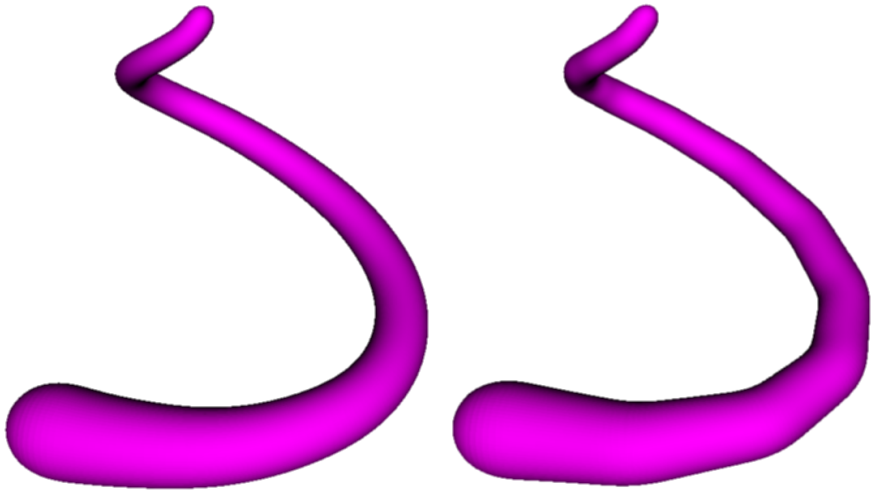

Figure 7: Convolution surface around an approximation of the spiral $(\frac{1}{2}t\cos t, \frac{3}{4}t\sin t, \frac{4}{5}t)$, $t \in [0, 2\pi]$. Left image: approximation with 14 arcs of circle; right image: approximation with 14 line segments.

great generality that draws from the use of recurrence formulae that were obtained with a new technique, creative telescoping.

This is nonetheless a first contribution in an ambitious project about convolution surfaces. The great advantage of convolution is indeed to provide a practical mathematical definition of a smooth surface around a complex skeletons made of intersecting curves and surfaces. Contrary to offset, sweep or canal surfaces, convolution surfaces naturally blend smoothly multiple primitive shapes. There are nonetheless challenges in their use. First the visualization mostly relies on refined marching cube algorithms. An alternative approach would be based on the prior construction of a *scaffold* around the skeleton as introduced in [19], with an alternative approach in [8]. A second challenge is the control of the topology and geometry. This problem was tackled in [24]. We expect to provide an alternative more intrinsic formulation, with mathematical guarantees.

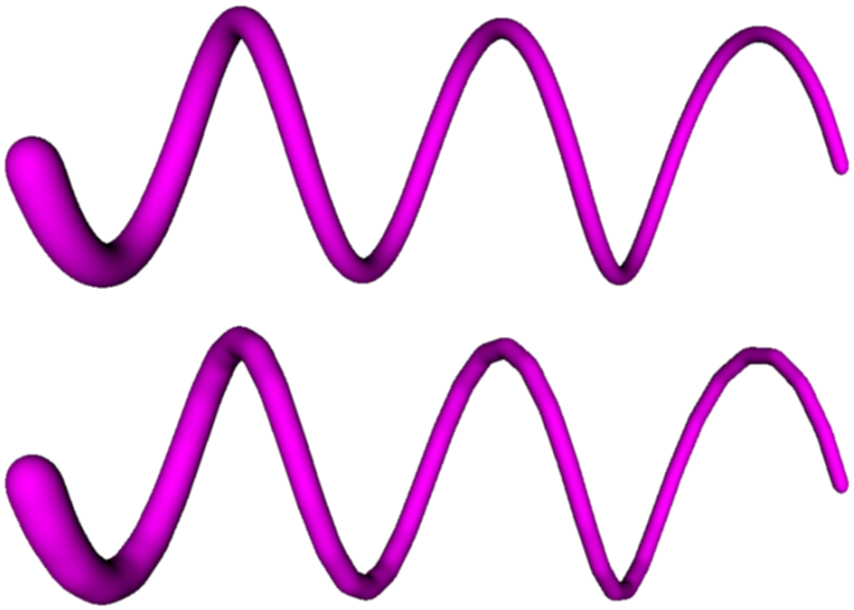

Figure 8: Convolution surface around an approximation of the elliptical helix $(2\cos t, 3\sin t, t)$, $t \in [0, 6\pi]$. Top image: approximation with 42 arcs of circle; bottom image: approximation with 42 line segments.

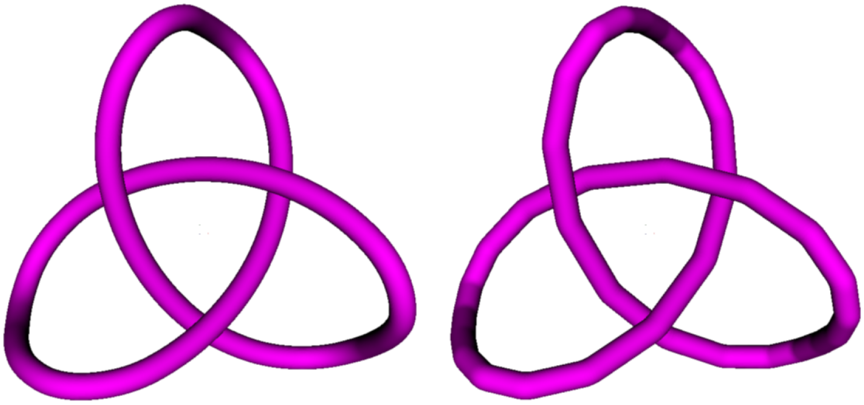

Figure 9: Convolution surface around an approximation of the closed curve $(-10\cos t - 2\cos 5t + 15\sin 2t, -15\cos 2t + 10\sin t - 2\sin 5t, 10\cos 3t)$, $t \in [0, 2\pi]$. Left image: approximation with 34 arcs of circle; right image: approximation with 34 line segments.

References

[1] Bertails, F., Audoly, B., Cani, M.-P., Querleux, B., Leroy, F., and Lévêque, J.-L. Super-helices for predicting the dynamics of natural hair. *ACM Transactions on Graphics 25*, 3 (2006), 1180.

[2] Blinn, J. F. A Generalization of Algebraic Surface Drawing. *ACM Transactions on Graphics 1*, 3 (1982), 235–256.

[3] Bloomenthal, J., and Shoemake, K. Convolution surfaces. *ACM SIGGRAPH Computer Graphics 25*, 4 (jul 1991), 251–256.

[4] Bostan, A., Dumont, L., and Salvy, B. Efficient Algorithms for Mixed Creative Telscoping. In *Proceedings of the ACM on International Symposium on Symbolic and Algebraic Computation* (New York, NY, USA, 2016), ISSAC '16, ACM, pp. 127–134.

[5] Bronstein, M. *Symbolic Integration I*, vol. 1 of *Algorithms and Computation in Mathematics*. Springer Berlin Heidelberg, Berlin, Heidelberg, 1997.

[6] Cani, M. P., and Hornus, S. Subdivision-curve primitives: A new solution for interactive implicit modeling. In *Proceedings - International Conference on Shape Modeling and Applications, SMI 2001* (2001), pp. 82–88.

[7] Chyzak, F. An extension of Zeilberger's fast algorithm to general holonomic functions. *Discrete Mathematics 217*, 1 (2000), 115–134.

[8] Fuentes Suárez, A. J., and Hubert, E. Scaffolding skeletons using spherical Voronoi diagrams. https://hal.inria.fr/hal-01509919/file/Fuentes17.pdf, Apr. 2017.

[9] Hornus, S., Angelidis, A., and Cani, M.-P. Implicit modeling using subdivision curves. *The Visual Computer 19*, 2 (2003), 94–104.

[10] Hubert, E. Convolution surfaces based on polygons for infinite and compact support kernels. *Graphical Models 74*, 1 (2012), 1–13.

[11] Hubert, E., and Cani, M.-P. Convolution surfaces based on polygonal curve skeletons. *Journal of Symbolic Computation 47*, 6 (2012), 680–699.

[12] Jin, X., and Tai, C.-L. Analytical methods for polynomial weighted convolution surfaces with various kernels. *Computers and Graphics 26* (2002), 437–447.

[13] Jin, X., and Tai, C. L. Convolution surfaces for arcs and quadratic curves with a varying kernel. *Visual Computer 18*, 8 (2002), 530–546.

[14] Jin, X., Tai, C.-L., Feng, J., and Peng, Q. Convolution Surfaces for Line Skeletons with Polynomial Weight Distributions. *ACM Journal of Graphics Tools 6*, 3 (sep 2001), 17–28.

[15] Jin, X., Tai, C.-L., and Zhang, H. Implicit modeling from polygon soup using convolution. *The Visual Computer 25*, 3 (2009), 279–288.

[16] Koutschan, C. A fast approach to creative telescoping. In *Mathematics in Computer Science* (2010).

[17] Milnor, J. W. Morse Theory. 153.

[18] Nutbourne, A. W., and Martin, R. R. *Differential geometry applied to curve and surface design*. John Wiley & Sons, 1988.

[19] Panotopoulou, A., Welker, K., Ross, E., Hubert, E., and Morin, G. Scaffolding a Skeleton.

[20] Sherstyuk, A. Interactive shape design with convolution surfaces. In *Shape Modeling International '99* (1999), pp. 56–65.

[21] Sherstyuk, A. Kernel functions in convolution surfaces: A comparative analysis. *Visual Computer 15*, 4 (1999), 171–182.

[22] Song, X., Aigner, M., Chen, F., and Jüttler, B. Circular spline fitting using an evolution process. *Journal of Computational and Applied Mathematics 231*, 1 (2009), 423–433.

[23] Wyvill, G., McPheeters, C., and Wyvill, B. Data structure for soft objects. *The Visual Computer 2*, 4 (1986), 227–234.

[24] Zanni, C. *Skeleton-based Implicit Modeling & Applications*. Phd, Université de Grenoble, 2013.

[25] Zanni, C., Bernhardt, A., Quiblier, M., and Cani, M.-P. SCALe-invariant integral surfaces. *Computer Graphics Forum 32*, 8 (2013), 219–232.

[26] Zanni, C., Hubert, E., and Cani, M.-P. Warp-based helical implicit primitives. *Computers and Graphics 35*, 3 (2011), 517–523.